

Self-Concatenated Coding and Multi-Functional MIMO Aided H.264 Video Telephony

Nasruminallah^{1,3}, Muhammad Fasih Uddin Butt^{2,3}, M. El-Hajjar³, Soon Xin Ng³, and L. Hanzo³

¹University of Engineering and Technology, Peshawar.

²COMSATS Institute of Information Technology, Islamabad, Pakistan.

³School of ECS, University of Southampton, SO17 1BJ, UK.

<http://www-mobile.ecs.soton.ac.uk>, Email: {1h}@ecs.soton.ac.uk

Abstract— Robust video transmission using iteratively detected Self-Concatenated Coding (SCC), multi-dimensional Sphere Packing (SP) modulation and Layered Steered Space-Time Coding (LSSTC) is proposed for H.264 coded video transmission over correlated Rayleigh fading channels. The self-concatenated convolutional coding (SECCC) scheme is composed of a Recursive Systematic Convolutional (RSC) code and an interleaver, which is used to randomise the extrinsic information exchanged between the self-concatenated constituent RSC codes. Additionally, a puncturer is employed for improving the achievable bandwidth efficiency. The convergence behaviour of the MIMO transceiver advocated is investigated with the aid of Extrinsic Information Transfer (EXIT) charts. The proposed system exhibits an E_b/N_0 gain of about 9 dB at the PSNR degradation point of 1 dB in comparison to the identical-rate benchmarker scheme.

I. MOTIVATION AND BACKGROUND

Bandwidth is a valuable commodity and therefore the information has to be transmitted over the communication channel as bandwidth-efficiently as possible. Therefore, the state-of-the-art multimedia coding standards primarily aim for a high compression efficiency [1]. However, the higher the coding efficiency, the more grave are the effects of transmission errors imposed on the video signal [2]. Hence, in order to protect the source coded stream from the effects of channel errors, powerful channel coding has to be applied, which introduces artificial redundancy in the source coded stream and is used for eliminating the channel-induced errors. Therefore, the error resilience is typically increased at the cost of a compromise in terms of coding efficiency.

The discovery of turbo codes made communications close to the Shannon limit feasible. The turbo principle of exchanging extrinsic information has been effectively utilised for diverse combinations of codes in order to improve the attainable error resilience. In recent years, intensive research efforts have been invested in the design of concatenated coding schemes, a philosophy, which was originally proposed by Forney [3]. The turbo principle of parallel concatenated convolutional codes (PCCCs or turbo codes) employs two or more constituent codes, which exchange extrinsic information in order to operate near the Shannon limit [4, 5], as detailed in [6].

Additionally, the limitations of wireless transmissions imposed by time-varying multipath fading can be mitigated using multiple-input multiple-output (MIMO) schemes [7]. More

The financial support of the following projects and organizations is gratefully acknowledged: University of Engineering and Technology Peshawar; COMSATS Institute of Information Technology Islamabad, Pakistan; the EU' CONCERTO Project; RC-UK under the auspices of the IU-ATC.

explicitly, information theoretic studies [8] have revealed that a MIMO system has a higher capacity than a single-input single-output (SISO) system. Substantial throughput improvements can be attained using a multi-layer MIMO structure designed for achieving a multiplexing gain, which is known as the Vertical Bell Labs Layered Space-Time (V-BLAST) scheme [9]. By contrast, a high transmit diversity gain can be achieved using Alamouti's low-complexity space-time code (STC) [10]. On the other hand, beamforming [11] provides an effective technique of reducing the multiple-access interference (MAI), where the antenna gain is increased in the direction of the target user, while reducing the gain towards the interfering users. In order to combine the benefits of the above-mentioned three MIMO schemes, we propose an amalgamated transmitter design, jointly exploiting the merits of V-BLAST, STC and beamforming, in order to achieve a high diversity gain, a high throughput as well as a beamforming gain. We referred to as a layered steered space-time code (LSSTC) [12]. Therefore, in this paper we offer a unified treatment of the topic of near-capacity multimedia transceivers, where we focus our attention on joint source and channel coding combined with LSSTCs and on the associated iterative decoding.

The rest of the paper is organised as follows. An overview of our system architecture is provided in Section II, while the video source stream is described in Section III. The performance of the proposed system is characterised with the aid of EXIT chart analysis in Section IV, while our overall performance results are presented in Section V. Finally, we offer our conclusions in Section VI.

II. SYSTEM OVERVIEW

A. Transmitter Model

The schematic of the proposed videophone arrangement is shown in Figure 1. At the transmitter side, the video sequence is compressed using the H.264/AVC video codec. Then, the output bit-stream representing a video frame consisting of K source coded bits x_k , $k = 1, 2, \dots, K$, is de-multiplexed into three different bit-streams, namely Stream A, Stream B and Stream C, containing the sequentially concatenated partitions of type A, B and C of all the slices per frame, respectively. The de-multiplexed binary output sequences x_a , x_b , and x_c , are then concatenated to form a bit-string s_1 , as shown in Figure 1, where we have $a = 1, 2, \dots, A$, $b = 1, 2, \dots, B$ and $c = 1, 2, \dots, C$, and $K = A+B+C$. The concatenated bit-string is subsequently protected by a rate-1/2 SECCC scheme which reduces the required chip-area, since it reuses a

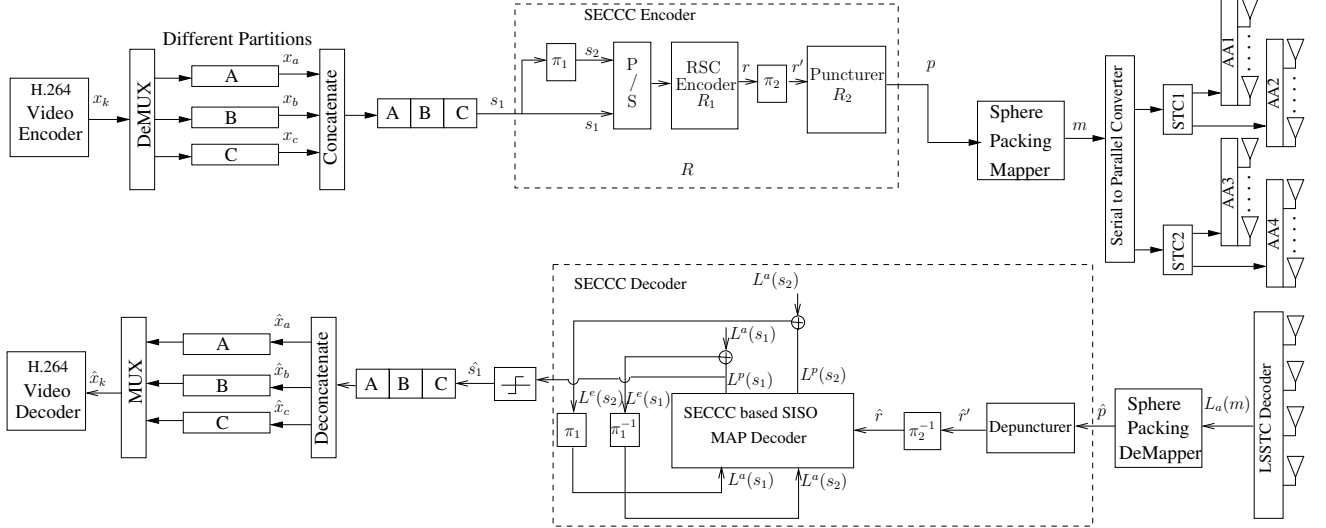


Fig. 1. The Proposed three-stage Iterative Source-Channel Decoding System Model.

single RSC constituent code in a 'self-concatenated' iterative manner. The attainable performance benefits relative to those of conventional RSC codes will be quantified in Section IV.

The input of the self-concatenated encoder is interleaved using the bit-interleaver Π_1 of Figure 1 to generate the bit-sequence s_2 . The employment of the interleaver Π_1 renders the information bits more-or-less uncorrelated. The resultant bit-sequences s_1 and s_2 are parallel-to-serial converted, before they are fed to the RSC encoder. More specifically, we used a rate $R_1 = 1/2$ RSC encoder having generator polynomials of $G_0 = 7, G_1 = 5$ and a memory of $v = 2$. The SECCC encoded bits r are interleaved using the random bit interleaver Π_2 of Figure 1, in order to randomise the coded bits. The interleaved bits r' are subsequently punctured using the rate $R_2 = 1/2$ puncturer of Figure 1. The employment of puncturing results in an increased bandwidth efficiency η , since it increases the effective code rate. Hence the overall code rate R_{total} can be calculated as:

$$R_{total} = \frac{R_1}{2 \times R_2} = \frac{1}{2} \left(\frac{1}{2(\frac{1}{2})} \right) = \frac{1}{2}. \quad (1)$$

Following puncturing, the resultant bits p are passed to the Sphere Packing (SP) modulator of Figure 1 [7]¹ and is subsequently transmitted with the aid of our LSSTC based transmission architecture.

The architecture seen in Figure 1 has transmit Antenna Arrays (AA), which are assumed to be spaced sufficiently far apart in order to encounter independent fading and hence to achieve transmit diversity. We note that owing to the large physical dimensions of this LSSTC architecture it is more appropriate for the downlink transmitter of the base station. Furthermore, the receiver is equipped with $N_r = 4$ receiver antennas, which is realistic for a laptop receiver. The so-called diversity product [7] of the LSSTC scheme is determined by the minimum Euclidean distance of all legitimate transmitted vectors. Therefore, the SP modulator provides the

benefit of jointly considering the space-time symbols of the LSSTC scheme, so that they are represented by a single phaser point selected from the SP constellation having the best known minimum Euclidean distance in the real-valued space. Since we invoke a twin-AA aided STC scheme, the SP design required is 4-dimensional. Assuming that there are L_{sp} legitimate vectors, the transmitter then has to choose the modulated signal from these L_{sp} legitimate symbols to be transmitted over the two AAs. More specifically, the SP modulator maps B number of coded bits $b = b_0, \dots, b_{B-1} \in \{0, 1\}$ to a SP symbol $v \in V$ so that we have $v = map_{sp}(b)$, where $B = \log_2(L_{sp})$, and L_{sp} represents the set of legitimate SP constellation points, as detailed in [7]. In this contribution, we considered $B = \log_2(16) = 4$ channel coded bits per SP symbol. Additionally, we consider transmission over a temporally correlated narrowband Rayleigh fading channel, associated with a normalised Doppler frequency of $f_D = f_d T_s = 0.01$, with f_d being the Doppler frequency and T_s the symbol duration.

B. Receiver Model

The transmitted signal is faded and contaminated by the additive white Gaussian noise (AWGN), hence the signal of $m' = hx + n$ is received, where h is the channel's non-dispersive fading coefficient and n is the AWGN having a variance of $N_0/2$ per dimension. The resultant signal is then fed into the soft-demapper in order to generate the conditional probability

$$P(m' | m^{(i)}) = \frac{1}{\pi N_0} \exp \left(-\frac{|m' - hm^{(i)}|^2}{N_0} \right) \quad (2)$$

of receiving m' , provided that $m^{(i)}$ was transmitted, where $i \in L_{sp} = \{0, 1, 2, \dots, 15\}$.

The resultant probability is then passed to the soft-depuncturer and the depunctured soft values are converted to bit-based Log-Likelihood Ratios (LLRs). Additionally, the puncturer inserts zero LLRs at the punctured bit-positions. The LLRs are then deinterleaved using the deinterleaver Π_2^{-1} of Figure 1 and are fed to the Soft-Input Soft-Output (SISO) maximum a-posteriori probability (MAP) decoder [13]. The self-concatenated decoder of Figure 1 iteratively exchanges extrinsic information, represented in the form of LLRs, to assist

¹The role of the SP scheme is to combine the conventional QPSK symbols of Alamouti's twin antenna based schemes into a joint SP symbol. The benefit of this is that this way we can jointly design the two antennas' space-time symbols, which allows us to improve the attainable diversity gain at the cost of an increased decoder complexity.

the SECCC decoder in approaching the $(1, 1)$ point of perfect convergence, in the EXIT-chart. The variable $L(\cdot)$ is used to represent the respective bit-LLRs, where the specific type of the LLRs is identified by the superscript a , p and e , corresponding to *a priori*, *a posteriori* and *extrinsic* information, respectively. Observe in Figure 1 that the extrinsic LLR $L^e(s_1)$ is generated by subtracting the *a priori* information $L^a(s_1)$ from the *a posteriori* LLR values $L^p(s_1)$ at the output of the SECCC based soft-input soft-output (SISO) MAP decoder, as shown in Figure 1. The LLRs $L^e(s_1)$ are then interleaved using the softbit interleaver Π_1 and are passed to the MAP decoder of Figure 1 in order to produce the *a posteriori* LLR values $L^p(s_2)$. Similarly, observe in Figure 1 that the *extrinsic* LLR values $L^e(s_2)$ of the bit sequence s_2 are obtained by subtracting the *a priori* information LLRs $L^a(s_2)$ input to the MAP decoder from the *a posteriori* LLRs $L^p(s_2)$. Following deinterleaving, these *extrinsic* LLRs $L^e(s_2)$ are fed back to the MAP decoder of Figure 1 as the *a priori* information $L^a(s_2)$. As seen in Figure 1 the *a priori* information $L^a(s_1)$ and $L^a(s_2)$ is exploited by the self-concatenated decoder for the sake of providing improved *extrinsic* information in the successive iterations. Self-concatenated decoding proceeds, until the affordable number of iterations is reached.

III. VIDEO SOURCE

The video source signal provided as the input of the proposed system seen in Figure 1 is generated by the H.264/AVC video source codec [2]. The *Akiyo* video test sequence of 45 frames represented in the Quarter Common Intermediate Format (QCIF) and consisting of (176×144) pixel resolution was encoded at 15 frames-per-second (fps) at a target bitrate of 64 kbps . In order to exploit frame slicing based partitioning, each frame was partitioned into 11-Macro-Block (MB) slices, resulting in 9 slices per QCIF frame. Two consecutive intra coded 'I' frames followed each other after 44 predicted or 'P' frames, which curtailed error propagation beyond the 45-frame boundary, i.e. beyond 3 seconds. Additional source codec parameters include the activation of the quarter-pixel motion estimation, intra-frame MB update options and the use of Universal Variable Length Coding (UVLC) type entropy coding. Furthermore, error resilience features such as Data Partitioned (DP) and intra-frame coded MB update of three randomly distributed MBs per QCIF frame were also incorporated. The insertion of bi-directionally predicted 'B' pictures results in unacceptable loss of lip-synchronisation owing to its delay and hence was avoided. Furthermore, the motion search was restricted to the immediately preceding QCIF frame in order to reduce the computational complexity of the video decoder. Similarly, the employment of Flexible Macro-block Ordering (FMO) was turned off, because despite its substantial increase in computational complexity it typically resulted in modest video performance improvements in low-motion video-telephony, using the "Akiyo" video test sequence, in order to keep the encoder complexity realistic for real-time implementation. The remaining system parameters of our experimental setup are listed in Table II.

TABLE I
CODE RATES FOR DIFFERENT ERROR PROTECTION SCHEMES

Error Protection Scheme	Code Rate		
	Outer Code	Inner code	Overall
SECCC Scheme	SECCC $R = \frac{1}{4}$	Puncturer $R_2 = \frac{1}{2}$	1/2
Benchmark Scheme	RSC $R = \frac{1}{4}$	Puncturer $R_2 = \frac{1}{2}$	1/2

TABLE II
SYSTEMS PARAMETERS

System Parameters	Value	System Parameters	Value
Source Coding	H.264/AVC	No of MB's/Slice	11
Source Bit-Rate	64Kbps	Intra-frame MB update/frame	3
Frame Rate	15fps		
No of Slices/frame	9		
Inner module	Puncturer	Over-all Code Rate	1/2
Modulation Scheme	SP	Channel	Correlated Rayleigh Fading
Number of Transmitter AA, N_t	4	Normalised Doppler Frequency	0.01
Number of Receiver Antennas, N_r	4		
Interleaver Length Π_1	$\approx (64000/15)$		

IV. ITERATIVE DETECTION AND EXIT CHART ANALYSIS

Iterative detection aided schemes [6] consist of a combination of two or more constituent encoders and interleavers. The principle of iterative detection using concatenated codes was first introduced in [3], but in the 1960s it was deemed to have an excessive computational complexity. After the discovery of turbo codes [5], which employed low-complexity RSC component codes, the implementation of low-complexity iterative decoding aided concatenated codes became a practical reality. The innovative iterative decoding of concatenated codes inspired researchers to extend this concept to numerous communication schemes in order to achieve high-integrity transmission of information [14].

EXIT charts [15, 16] are widely used for the analysis of iterative receivers by providing an insight into the convergence behaviour of the system based on the exchange of mutual information amongst the constituent receiver components. They analyse the input/output mutual information characteristics of the SISO decoder's *a priori* and *extrinsic* LLR values with respect to the corresponding bit-decisions. More explicitly, for the symbol s having an *a priori* LLR value of $L^a(s)$, the mutual information (MI) is denoted by $I_A(x)$, while the MI between the *extrinsic* LLR $L^e(s)$ and the corresponding symbol x is denoted by $I_E(x)$. The EXIT charts are capable of successfully predicting the SNR, where the turbo-cliff region of the BER curve is expected to be for a concatenated code. This is achieved by identifying the E_b/N_0 value, which results in an open EXIT-chart tunnel between the EXIT curves of the corresponding constituent components. According to the EXIT chart analysis of iterative decoding, an infinitesimally low BER can only be achieved by an iterative receiver, if there exists an open EXIT tunnel between the two constituent decoders EXIT curves, so that during the process of iterative decoding, the constituent decoders reach the highest possible extrinsic information of $I_E = 1$, when provided with perfect *a priori* information, as shown in Figure 2.

The EXIT charts recorded for the binary SECCC scheme of Table I are shown in Figure 2. The two curves represent the two hypothetical decoder components of the self-

concatenated scheme. Since they are identical components, we only computed the EXIT curve of a single component, while the other is its mirror image with respect to the diagonal line. The stair-case shaped function corresponds to the Monte-Carlo simulation based decoding trajectories of the proposed system at the E_b/N_0 values of -2 , -1 and 0 dB, respectively. The reason for plotting the EXIT chart together with the corresponding decoding trajectory is to visualise the iteration-by-iteration transfer of extrinsic information between the decoder components.

According to Figure 2, the EXIT curve of the combined SISO module constituted by the SECCC scheme cannot reach the $(1, 1)$ point of perfect convergence in the EXIT chart at the E_b/N_0 value of -2 dB, since the two curves intersect and hence they are unable to provide an open EXIT tunnel. This implies that an infinitesimally low BER cannot be achieved. However, it may be observed from the decoding trajectories of Figure 2 that for an E_b/N_0 value of 0 dB or higher the SECCC scheme becomes capable of achieving the highest possible extrinsic information of $I_E = 1$ during the iterative decoding process.

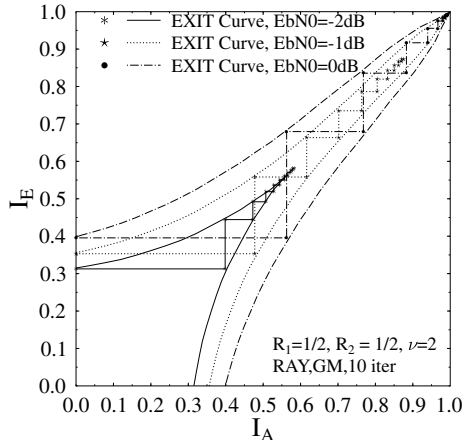


Fig. 2. The EXIT chart and simulated decoding trajectories for the SECCC scheme associated with $R_1 = 1/2$, $R_2 = 1/2$ at $E_b/N_0 = 0$, -1 and -2 dB, for transmission over correlated Rayleigh fading channel using SP modulated LSSTC.

In order to verify the EXIT chart based convergence prediction, the Monte-Carlo simulation-based bit-by-bit decoding trajectory recorded by acquiring the mutual information at the constituent decoders is used at the E_b/N_0 values considered, as presented in Figures 2. Observe from the decoding trajectories of Figure 2 that for E_b/N_0 values higher than 0 dB the SECCC-LSSTC-SP scheme becomes capable of achieving the highest possible extrinsic information of $I_E = 1$ during the iterative decoding process.

V. SYSTEM PERFORMANCE RESULTS

In this section we present our overall performance results for the proposed system. We consider the SP modulation scheme [7] associated with $L = 16$ sphere-packing modulated symbols for the bits-to-SP symbol mapping. The performance of the system was evaluated, while considering various combinations of the self-iterations It_{self} . For the sake of increasing the confidence in our results, we repeated each 45-frame based video-session 160 times and averaged the generated results.

The BER performance of the error protection scheme employed is shown in Figure 3. It can be observed from Figure 3, that as expected the SECCC-LSSTC-SP scheme using $It_{self} = 10$ self-iterations results in the best BER performance, when compared to $It_{self} = 2$ and 3 self-iterations for the specific error protection scheme considered. Additionally, it can be seen that the benchmarker RSC-LSSTC-SP scheme results in the worst BER performance due to its inability to perform self-iterations. Hence this scheme fails to reach the $(1,1)$ point of perfect convergence.

Furthermore, the $PSNR$ versus E_b/N_0 curve of the proposed error protection scheme is portrayed in Figure 4. It may be observed in Figure 4 that the SECCC-LSSTC-SP scheme employing rate- $\frac{1}{2}$ SECCC and $It_{self} = 10$ self-iterations results in the best $PSNR$ performance across the entire E_b/N_0 region considered. It is also observed in Figure 4 that when performing iterative decoding, while employing the RSC benchmark codes results in the worst $PSNR$ performance at the same overall code rate of $\frac{1}{2}$, as given in Table I. Quantitatively, when using the SECCC-LSSTC-SP scheme of Table I, an E_b/N_0 gain of upto 9 dB may be achieved relative to the identical-rate RSC-LSSTC-SP benchmarker scheme at the $PSNR$ degradation point of 1 dB, as shown in Figure 4.

Additionally, in order to analyse the effects of different motion activities on the performance of the video transceiver architecture setup of Figure 1, we considered diverse video test sequences, such as the "Akiyo", "News" and the "Foreman" clips. The test sequences considered were encoded using the H.264/AVC codec, while considering the system parameters of Table II. Again, we utilised the system architecture of Figure 1, while considering the parameters of Table II. It can be observed by viewing these video sequences that the "News" video sequence has a higher motion activity than the "Akiyo" video sequence. Similarly, the "Foreman" video sequence has a higher motion activity than the "News" video clip. The BER versus E_b/N_0 performance of the video test sequences considered is presented in Figure 3. It can be observed from Figure 3 that -as expected- the resultant BER versus E_b/N_0 performance is the same, regardless of the video test sequences considered. Similarly, the $PSNR-Y$ versus E_b/N_0 performance of the "Akiyo", "News" and the "Foreman" video test sequences is shown in Figure 4. It can be observed from Figure 4 that the objective video quality of the low bit-rate video coding configuration of Table II is dependent on the amount of motion activity within the video scene. The "Akiyo" video sequence associated with the lowest motion activity has the best $PSNR$ performance. Similarly, due to the high motion activity of the "Foreman" video sequence, the less motion-active "News" video sequence has a better objective video quality than the "Foreman" sequence in the E_b/N_0 range considered in Figure 4.

Finally, the subjective video quality of the error protection schemes employed is characterized in Figure 5. The video frames presented in Figure 5 were obtained by repeated retransmission of both the luminance and chrominance components of the *Akiyo* video sequence using the same system in conjunction with $It_{self} = 10$ self-iterations 30 times, in order to have a pertinent subjective video quality comparison.

Observe from Figure 5 that an acceptable video quality is attained by the SECCC-LSSTC-SP scheme at an E_b/N_0 value of 0 dB. However, video impairments persist for the RSC-LSSTC-SP scheme even at the relatively high E_b/N_0 values of 6 dB, 7 dB, 8 dB and 9 dB, as shown in Figure 5.

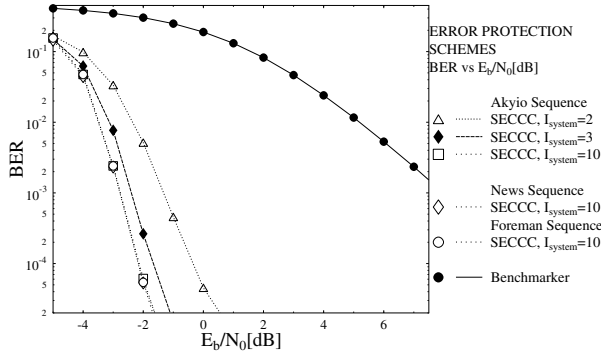


Fig. 3. BER vs E_b/N_0 performance of the various error protection schemes summarised in Table I.

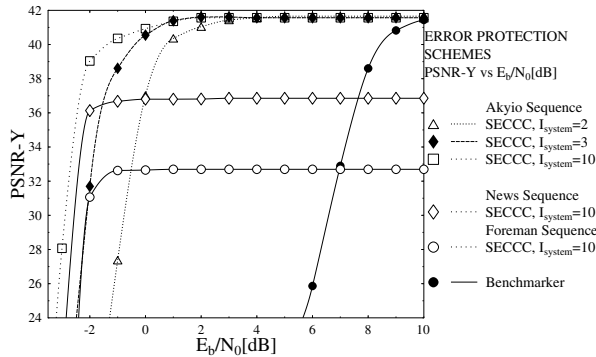


Fig. 4. PSNR-Y vs E_b/N_0 performance of various error protection schemes summarised in Table I.

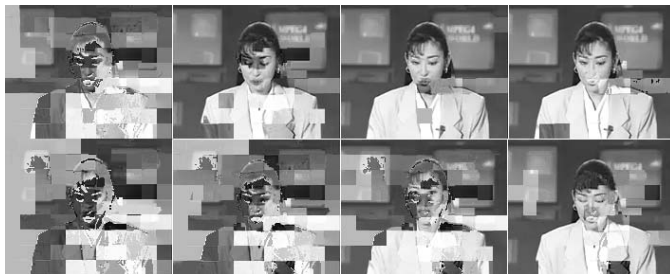


Fig. 5. Subjective video (cumulative error) quality of the 45th "Akiyo" video sequence frame using (from top) LSSTC-SP-SECCC and benchmarker schemes summarised in Table I at E_b/N_0 values of (from left) -3 dB, -2 dB, -1 dB and 0 dB for LSSTC-SP-SECCC and 6 dB, 7 dB, 8 dB and 9 dB for the benchmarker RSC-LSSTC-SP scheme.

VI. CONCLUSIONS

In this contribution we presented a low complexity near-capacity channel coding system design constituted by self-concatenated convolutional coding (SECCC), for the transmission of H.264 source coded video streams. Additionally, LSSTC aided multi-dimensional SP modulation was invoked, which was designed for near-capacity multimedia transmission. Our multi-functional LSSTC scheme combines the ben-

efits of STC, V-BLAST as well as beamforming. The employment of EXIT-chart optimised SECCC, which deliberately imposed artificial redundancy on the source coded bit stream provided significant improvements in terms of the *PSNR* versus E_b/N_0 performance, when compared to the benchmarker scheme employing an equivalent-rate RSC code. Additionally, the convergence behaviour of the proposed system was analysed with the aid of EXIT charts. Our H.264/SECCC/LSSTC-SP based design example exhibited an E_b/N_0 gain of 9 dB at the PSNR degradation point of 1 dB relative to the identical-rate benchmarker. Our future work will focus on the design of a SECCC based three-stage architectures design constituted by serially concatenated and iteratively decoded short block codes (SBCs), SECCC and a multi-dimensional sphere packing (SP) modulation scheme, operating closer to capacity, while maintaining a high bandwidth efficiency.

REFERENCES

- [1] D. Marpe, T. Wiegand, and G. J. Sullivan, "The h.264/MPEG4 advanced video coding standard and its applications," *IEEE Communications Magazine*, vol. 44, pp. 134–143, Aug. 2006.
- [2] L. Hanzo, P. Cherriman, and J. Streit, *Video Compression and Communications: From Basics to H.261, H.263, H.264, MPEG2, MPEG4 for DVB and HSDPA-Style Adaptive Turbo-Transceivers*. Wiley-IEEE Press, 2007.
- [3] G. Forney, "Concatenated codes," *MIT Press, Cambridge*, 1966.
- [4] C. E. Shannon, "A mathematical theory of communication," *The Bell System Technical Journal*, vol. 27, pp. 379–423,623–656, July 1948.
- [5] C. Berrou, A. Glavieux, and P. Thitimajshima, "Near shannon limit error-correcting coding and decoding:turbo-codes. 1," in *IEEE International Conference on Communications*, vol. 2, (Geneva, Switzerland), pp. 1064–1070, May 1993.
- [6] L. Hanzo, T. H. Liew, and B. L. Yeap, *Turbo Coding, Turbo Equalisation and Space-Time Coding for Transmission over Fading Channels*. New York, NY, USA: John Wiley & Sons, 2002.
- [7] L. Hanzo, O. Alamri, M. El-Hajjar, and N. Wu, *Near-Capacity Multi-Functional MIMO Systems : Sphere-Packing, Iterative Detection and Cooperation*. New York, NY, USA: John Wiley & Sons, 2009.
- [8] N. Chiurtu, B. Rimoldi, and E. Telatar, "On the capacity of multi-antenna Gaussian channels," in *Information Theory, 2001. Proceedings. 2001 IEEE International Symposium on*, (Washington, DC, USA), 2001.
- [9] P. W. Wolniansky, G. J. Foschini, G. D. Golden, and R. A. Valenzuela, "V-BLAST: an architecture for realizing very high data rates over the rich-scattering wireless channel," in *Signals, Systems, and Electronics, 1998. ISSSE 98. 1998 URSI International Symposium on*, (Pisa, Italy), pp. 295–300, Sept./Oct. 1998.
- [10] S. M. Alamouti, "A simple transmit diversity technique for wireless communications," *IEEE Journal on Selected Areas in Communications*, vol. 16, no. 8, pp. 1451–1458, 1998.
- [11] J. Blogh and L. Hanzo, *Third-generation systems and intelligent wireless networking: smart antennas and adaptive modulation*. John Wiley & Sons - IEEE Press, 2008.
- [12] M. F. U. Butt, R. A. Riaz, S. X. Ng, and L. Hanzo, "Near-capacity iteratively decoded binary self-concatenated code design using EXIT charts," in *IEEE Global Communications Conference, GLOBECOM '08*, (New Orleans, USA), Nov./Dec. 2008.
- [13] S. Benedetto, D. Divsalar, G. Montorsi, and F. Pollara, "Serial concatenated trellis coded modulation with iterative decoding," in *Information Theory, 1997. Proceedings., 1997 IEEE International Symposium on*, (Ulm, Germany), June/July 1997.
- [14] D. Divsalar and F. Pollara, "Multiple turbo codes for deep-space communications," *Telecommunications and Data Acquisition Progress Report, Jet Propulsion Laboratory, (Pasadena, CA)*, pp. 42–121, 15 May 1995. <http://hdl.handle.net/2014/3115>.
- [15] S. ten Brink, "Designing iterative decoding schemes with the extrinsic information transfer chart," in *AEU International Journal of Electronics and Communications*, vol. 54, pp. 389–398, Nov. 2000.
- [16] S. ten Brink, J. Speidel, and R.-H. Yan, "Iterative demapping and decoding for multilevel modulation," in *Global Telecommunications Conference, 1998. GLOBECOM 98. IEEE*, vol. 1, (Sydney, NSW, Australia), pp. 579–584, 1998.